Environmental Engineering Research

Environ. Eng. Res. 2013 December,18(4) : 211-219

Review Paper

http://dx.doi.org/10.4491/eer.2013.18.4.211
pISSN 1226-1025 eISSN 2005-968X

Environmental Applications of Rare-Earth Manganites as Catalysts: A Comparative Study

D. Alami†

Department of Inorganic Substances Technology, National Techical University "Kharkiv Polytechnic Institute", Kharkiv 61002, Ukraine

Abstract

Rare-earth manganites have a great potential for environmental applications based on their chemical and physical properties. The use of rare-earth manganites as catalysts for environmentally essential reactions was reviewed. Artificial neural networks were used to assess the catalytic activity in oxidation reactions. Relative catalytic activities of the catalysts were further discussed. We concluded that cerium manganite is the most practicable catalyst for technological purposes.

Keywords: Artificial neural networks, Catalytic activity, Enthalpy of formation, Environmental catalysis, Rare-earth manganites

1. Introduction

Research in environmental catalysis has continuously evolved over the last two decades owing to the necessity of obtaining worthwhile solutions to environmental pollution problems. The development of innovative environmental catalysts is a crucial factor towards the purpose of determining new sustainable manufacturing technologies. Substantial enlargement of the traditional field of environmental catalysis also took place in the last decade [1].

Perovskite-type oxides of general formula ABO_3 attract notable attention of explorers due to their high catalytic activity in numerous redox reactions. The perovskites have been applied in the selective reduction of nitric oxide with propene, in the oxidation of CO and hydrocarbons, reduction of NO and CO. Other applications, such as methane combustion, oxidative coupling of alkanes, hydrogenation and hydrogenolysis of hydrocarbons, and ammonia oxidation, show the importance of perovskite-type oxides. The aforementioned oxides are capable of including different metal cations in their crystalline structure [2] (Fig. 1). Their properties strongly vary, depending on the A and B ions' nature and oxidation states. The ion A (rare-earth) in the majority of cases is catalytically inactive and merely provides thermal stability, while ion B (transition metal) is the active component. The effect of the partial replacement of cation A with elements that have the identical oxidation state has been generally studied, while the influence of the B cation's replacement, and its use in catalytic oxidation has attracted less attention [3].

In comparison with constituent oxides, perovskites are reported to be better catalysts for pollution control. Partial changing of A or B cations to those that include different oxidation states, leads to oxygen vacancies formation or suppression in the catalysts; this fact allows the enhancing of catalytic activity. In this process, the native structure of the perovskite will not be changed [4]. Thus, the study of the effect of the A-site cation on the catalytic activity of the perovskites would be attractive. In the present investigation, there is an attempt to perform the comparative study of catalytic activity of the manganites with different rare-earth A-site cations in oxidation reactions, which have strong environmental impact, or would have it in the near future.

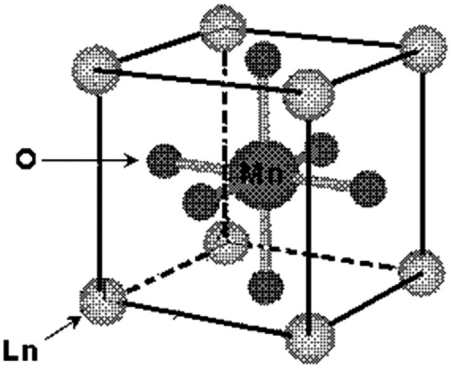

Fig. 1. $LnMnO_3$ ideal perovskite structure.

Received May 01, 2013 **Accepted** August 01, 2013

†Corresponding Author
E-mail: david.alami@gmail.com
Tel: +380937687573 Fax: +380577076241

2. Environmental Applications of Rare-Earth Manganites

The use of perovskite-type oxides as catalysts for high temperature combustion (gas turbine, catalytic burners) is particularly interesting due to their thermochemical stability in the atmosphere containing oxygen and steam at high temperatures [5]. However, the catalytic system must be adequately shaped to achieve mechanical strength and chemical stability. There was an attempt [6] to form rings of different perovskites without any addition of binders or peptizers, but these rings showed low mechanical strength. An option is to deposit a catalytic component on a support, which satisfies some criteria. It should be noted that an important advantage of catalytic combustion is to reduce the formation of NO at the source, the reason being the sharp decrease in the appearance of high temperature spots typical for non-catalytic combustion. In principle, the presence of a reducing agent should speed up the "cleaning" of the catalyst surface. Of course, this is a reasonable conclusion if the same mechanism operates in the presence of the reducing agent, if it is CO or hydrocarbons [5].

Among the $LnMnO_3$ materials, the lanthanum manganite ($LaMnO_3$) shows high thermal stability and oxygen mobility. The compound was studied extensively in catalytic oxidation of several volatile organic compounds (VOC). Oxidation of acetone, isopropanol and benzene in the presence of $LaMnO_3$ perovskite was studied in recent work [7]. The activity decreases from acetone to benzene. Lanthanum manganite has also been applied to the destruction of chlorinated VOC, methanol and presents activity in nitrogen oxides reduction [8].

The results of complete destruction of VOC like C_1 (CH_3Cl, CH_2Cl_2, $CHCl_3$ and CCl_4) and C_2 (CH_3-CH_3, CH_2Cl-CH_2Cl) molecules [9] showed that it could be achieved in the air below 550°C over $LaMnO_3$ catalysts. However, the formation of by-products, such as C-C coupling, higher chlorinated and cracking compounds, involves catalytic deactivation. The $LaMnO_3$ perovskite-type catalysts are rarely investigated in the field of hydrocarbon VOC abatement.

It is considered that some factors, such as morphology (including microstructure, crystalline phase, and specific surface area), redox properties (including the low-temperature reducibility and the nature of the redox couple) and surface chemical species (including adsorbed oxygen, the amount of B-site cations or oxygen vacancies), determine the catalytic activity of $LaMnO_3$ perovskite-type materials in the oxidation reaction [9], many researchers focused their efforts on understanding those effects with the objective to improve the catalytic performances. For example, three-dimensionally ordered macroporous perovskite $LaMnO_3$ was prepared using the templating method with surfactant addition [10]. The surfactant influenced the pore structure of $LaMnO_3$ material and allowed achieving a high surface area. Results showed that the catalytic performance of the porous $LaMnO_3$ sample was superior to the bulk counterpart for toluene oxidation. In order to improve redox properties, the B-site substituted $LaMnO_3$ perovskite with Pd, Pt, and Rh was studied for methanol partial oxidation [11]. The authors showed that significant promotion of reducibility and oxygen activity were achieved for $LaMn_{0.95}B_{0.05}O_3$ compared to the untainted $LaMnO_3$ catalysts. Consequently, the $LaMn_{0.95}B_{0.05}O_3$ exhibits higher reactivity than pure $LaMnO_3$. It was suggested [12], that in the $LaMnO_3$ perovskite oxide, Mn^{4+}/Mn^{3+} redox couple plays the key role in the catalytic oxidation of VOC. Substitution of B-site with Co, Ni, and Fe generated more Mn^{4+} species, enhancing the redox ability of the Mn^{4+}/Mn^{3+} couple, created more oxygen vacancies, increasing the oxygen mobility and involving more adsorbed oxygen species, which are considered as the most active species for the catalytic oxidation reaction.

The possibility of catalytic activity enhancement in NO reduction was also studied [13]. They prepared Ce-doped $PrMnO_3$ catalysts and studied the effect of cerium doping on their catalytic properties. The results obtained showed that in the case of the Ce-doped series with lower doping ratio, most of the Ce^{4+} ions were introduced into the A-site to form perovskite-type oxides with some additional ceria. It was shown that the oxidation state of manganese was more easily affected by the addition of cerium and more vacancies might arise at the A-site due to the structural limit of the oxide. High catalytic activity in NO reduction might be caused by the presence of oxygen vacancies and the relative ease of oxygen removal. Besides, ceria could adsorb oxygen to sustain the reduction of NO. For higher Ce-doped samples, it was proposed to develop some Pr-substituted CeO_2–MnO_x solid solutions. The addition of ceria into manganese oxides increased the quantity of oxygen desorption by partial reduction of manganese. It was also reported [14] that the doping of Mn strongly influenced the redox behavior of the ceria based solid solutions by promoting the low-temperature reduction of Ce^{4+}. According to these observations it was suggested that the formation of CeO_2–MnO_x solid solutions further enhanced the oxidative/reductive property of the catalyst largely based on the reversible adsorption/desorption cycles of lattice oxygen.

Catalytic activity of the samples of nanosized perovskite-type complex oxide samples $AMnO_3$ (A = La, Ce, Pr, Nd; B = Mn, Co, Fe, Ni, Cr) was tested for simultaneous removal of soot particles and NO_x [15]. Kinetic measurements were performed by a technique of temperature-programmed reaction. It was shown that different ions at the B-site in $LaBO_3$ perovskite-type oxides have strong effects on their catalytic performances for the coincident removal of soot and NO. The temperature order of soot combustion from high to low follows: $LaCoO_3 > LaNiO_3 > LaMnO_3 > LaFeO_3 > LaCrO_3$; the order of NO conversion is: $LaCrO_3 > LaMnO_3 > LaCoO_3 > LaFeO_3$. The temperature order of soot combustion from low to high is: $LaMnO_3 > NdMnO_3 > CeMnO_3 > PrMnO_3$. When Mn^{3+} in the $LaMnO_3$ was partially substituted by the lower valence cation (K^+, Cs^+, Sr^{2+}), according to the principle of electron neutrality, the positive charge reduced could be balanced, either by the increase of oxygen vacancy or the formation of higher oxidation state ion at the B-site, and the B^{3+}–B^{4+} system was formed. The increase of oxygen vacancy and the B^{3+}–B^{4+} system in perovskite-type complex oxides largely improved their redox activities. When Mn^{3+} in the $LaMnO_3$ was partially substituted by transition metal, due to the cooperation of two ions in the B site, the catalytic activities for the simultaneous removal of soot and NO exhausted from a diesel engine were noticeably improved. The transition metals Cu^{2+} and Co^{3+} were found as the best replacers.

The study of the kinetics of the decomposition of nitrous oxide on a series of isostructural ternary oxides of the general formula $LnMnO_3$ (where Ln = La, Nd, Sm, or Gd) was reported by Raj and Srinivasan [16]. In this work an evaluation of the catalytic activities of these compounds for oxidation reactions was performed. A correlation of catalytic activity with lattice parameters was found. During the investigation, it was shown that the decomposition of N_2O should primarily involve the desorption of oxygen as the rate-determining step. The order of catalytic activ-

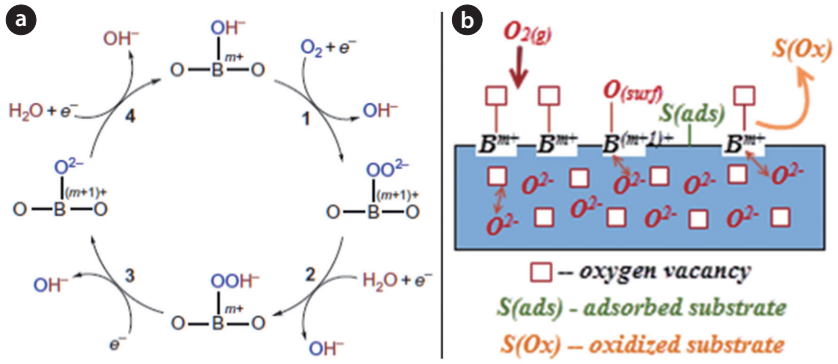

Fig. 2. Mechanism of oxidation-reduction reactions on perovskite oxides: a) aqueous solution and b) gas phase.

ity from high to low is as follows: $LaMnO_3$ > $SmMnO_3$ > $NdMnO_3$ > $GdMnO_3$.

The catalytic activities of $LnBO_3$ (B = Cr, Mn, Fe, Co, Ni) were studied for propene oxidation at 230°C to evaluate the effect of the A- and B-site elements. It was observed that the specific activities decreased according to $LnCoO_3$ > $LnMnO_3$ > $LnNiO_3$ > $LnFeO_3$ > $LnCrO_3$. Similar results were reported for C_3 and C_4 oxidation over $LaBO_3$, (B = Cr, Mn, Fe, Co, Ni), showing that the transition metal in the B-site plays a crucial catalytic role as an active site. Co and Mn are the most active 3d-transition metals. The role of the lanthanides is secondary, as long as they are trivalent [17].

Arai et al. [18] studied the catalytic behavior of $LaBO_3$ (B = Co, Mn, Fe, Cu, Ni, Cr) for methane combustion compared to Pt(l%)/Al_2O_3. The temperature at which the conversion of methane was 50% was used to estimate the catalytic activity. Co, Fe and Mn based perovskites were the most active in this series. Their activities were pretty close to that of Pt(l%)/Al_2O_3.

$La_{0.8}Sr_{0.2}MnO_3$ was tested as a catalyst for combustion of acetone and compared to $CuMn_2O_4$, The later solid is a commercial catalyst for VOCs removal. The perovskite was more effective than the copper manganate [19].

Much attention has been given to cerium manganite for a number of catalytic applications, especially in pollution control. This compound is known to be effective for catalytic wet oxidation of phenol [20] and formaldehyde. Lately, $CeMnO_3$ has been shown to cause a significant lowering of diesel soot oxidation temperature and to be selective for catalytic reduction of NO_x with ammonia. It has been reported that the MnO_x–CeO_2 mixed oxides showed high activity and stability in the catalytic combustion of trichloroethylene and chlorobenzene. Cerium manganite has also been suggested to have a potential for hydrogen production by the two-step splitting of water [21].

The reaction mechanism of catalytic oxidation with oxygen in alkaline aqueous solution in Fig. 2(a) proceeds via four steps [22]: 1) surface hydroxide displacement; 2) surface peroxide formation; 3) surface oxide formation; and 4) surface hydroxide regeneration. The catalytic activity of the investigated perovskites in oxidation reaction of VOCs in gas phase correlates well with the amount of the active oxygen species (O^{2-}, O_2^-, O^-) determined by the structural defects generated by the Mn^{4+}/Mn^{3+} ratio in the perovskite structure [23]. The interaction of surface oxygen species with reactants constitutes the suprafacial mechanism of gas phase oxidation perovskite catalysts in Fig. 2(b). More oxygen vacancies involve a larger density of adsorbed surface oxygen species, which are further available for substrate oxidation. Additionally, the formation of oxygen vacancies favors the lattice oxygen mobility, which can directly affect the catalytic activity [24].

We must admit that the catalytic activity of praseodymium, europium and gadolinium manganites has been less studied. These compounds, as well as lanthanum manganite, were tested for carbon monoxide and methanol oxidation. The reported order of activity decreases in the following series La > Pr > Eu > Gd [24].

After this brief review of perovskite applications, we conclude that the use of these and related mixed oxides in combustion is already established and has reached in some cases, commercial status. Many potential applications have also been reported in the patent literature. Turning attention to the academic media, one sees many attempts to find new uses of these compounds in NO_x abatement, catalytic combustion, syngas production and other miscellaneous, albeit interesting, applications.

There are three main points that require much effort if new commercial applications of these materials are to be achieved. They are [3]:

1) The development of new methods or improvement of existing ones to prepare supported mixed oxides.
2) The production of membranes containing active perovskite materials.
3) The study of chemical transformations under conditions remarkably close to those found in practice.

The latter statement is illustrated by a traditional situation occurring in environmental catalysis. The exhaust gases from different types of engines usually contain high concentrations of water vapor and SO_2. Therefore, any realistic approach to the development of catalysts to eliminate pollutants from these streams needs to include SO_2 and water in the feed of the experimental reactors. In brief, we believe that there are many potential practical applications for these materials that will be fully realized in the near future.

Thorough analysis of reference literature shows that no experimental investigations for potentially catalytically active terbium, thulium, and holmium manganites have been conducted to date. Moreover, there is a lack of comparison studies concerning catalytic activity of abovementioned manganites. The main goal of the present study is to compare catalytic activity of different rare-earth manganites in oxidation reactions.

3. Relationships between Structure, Composition, and Catalytic Activity

Knowledge of the relationships between solid state properties and the catalytic activity is essential for the development of efficient catalysts. The availability of data on the families of isostructural perovskite oxides is particularly valuable to look for these relationships. By changing the cation A, while keeping steady cation B, or conversely, a series of compounds can be synthesized with no principal change in the crystal structure [3].

Besides practical applications, numerous key reviews have been completed clarifying the relationship between solid state chemistry and catalysis of perovskites. A generalization of this works leads to the following principles [25]:

1) There are various combinations of A and B cations that yield perovskite-type oxides (ABO_3). In addition, partial replacement of particular cations is nearly always achievable without disturbing the native crystal structure.
2) Proper combinations and partial replacement of A- and B-site cations give rise to irregular valence of B-site positive holes and vacancies of oxide ions. Introduction of such lattice defects cause changes to the chemical or transport properties of the oxides, and this affects the catalytic performance.

In the research field of oxidation reactions over perovskite oxides, Voorhoeve et al. [26] proposed two types of oxidation mechanism. The first one was interfacial reactions in which lattice oxygen acts as the active species, and the second one was suprafacial reactions in which adsorbed oxygen acts as the active species. The suprafacial mechanism was assumed to occur in the low temperature range, at which an adsorption-desorption equilibrium of oxygen was thermodynamically maintained. With temperature increasing, the concentration of surface adsorbed oxygen decreased, and the lattice oxygen became more mobile and participated in the oxidation reactions. This implied a gradual transition from the suprafacial mechanism to the interfacial mechanism. Using this reasoning, Voorhoeve et al. [26] suggested that the oxidation of CO at temperatures below 350°C over the perovskites of 3d transition metals is an example of suprafacial catalysis, whereas the reduction of NO with CO and H_2 over the aforementioned oxides is an example of intrafacial catalysis. From the standpoint of oxygen species involved in the catalysis, adsorbed, surface and lattice oxygen seem to provide for suprafacial and intrafacial catalysis, respectively. In fact, it was reported that, in the methane oxidation over $La_{0.8}Sr_{0.2}MnO_3$, weakly bonded adsorbed oxygen acted at lower temperatures, while lattice oxygen became active at higher temperatures.

The concept of suprafacial and intrafacial catalysis is quite empirical. Which mechanism is suitable can depend on the composition and B-site metal perovskite [25]. With some precision, it can be said that unsubstituted perovskites ABO_3 tend to catalyze the suprafacial reaction. Among A-site substituted oxides, Co- and Fe-perovskites catalyze the intrafacial reaction, while Mn-perovskites act on the suprafacial reactions. It is estimated that the difference between the suprafacial and intrafacial catalyst is entirely linked to the facility of migration of oxide ions. Mobile oxide ions in the subsurface layers have a possibility to participate in catalysis. Conversely, if oxide ions are not mobile, the suprafacial mechanism would predominate. Such a consideration suggests the relevance of a defect structure in the catalysis of perovskites.

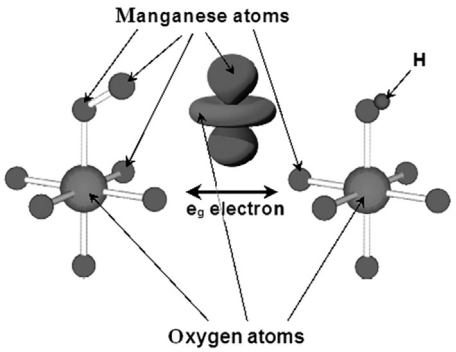

Fig. 3. The shape of the e_g electron points directly towards the surface O atom and plays an important role during O_2^{2-}/OH^- exchange.

It is now clear that the most frequently used rare-earth manganites are not of the simple ABO_3 type but are complex oxides with A or B sites that can be partially substituted. It seems relevant to learn first the importance of such partial substitution in the context of solid-state chemistry.

While studying nitrous oxide decomposition on a series of isostructural rare-earth manganites the researchers [16] obtained a linear relationship, indicating the increase of activation energy with the increase of the cell constant. When the cell constant increases, the Mn-O bond length increases as well, thereby weakening the Mn-O bond and increasing the d electron density around the Mn ion. This fact would result in a strong interaction between the transition metal ion and the adsorbed oxygen. An increase in the cell constant also increases the distance between two adjacent Mn ions, making the process of getting two ions sufficiently near to each other to make desorbing O_2 comparatively difficult. From the above arguments, it is evident that desorption of oxygen should be the rate-determining step in the decomposition reaction. The decomposition of nitrous oxides has been shown to be a suprafacial reaction, where the catalyst enters the reaction as a relatively inert template providing a collection of atomic orbitals of appropriate symmetry and energy. The relevant energy levels are those around the Fermi level, i.e., the lowest unoccupied and the highest occupied levels. In the case of these manganites, the electronic configuration is primarily dependent on the 3d levels of Mn ions and the p orbitals of oxygen. The Mn ions have to provide the empty d orbitals of appropriate symmetry to overlap with filled p orbitals of oxygen (for electron transfer) in the desorption step. For Mn, these orbitals are d_{z2} and d_{x2-y2}. As one proceeds from lanthanum to gadolinium, the electrons are being filled up successively and therefore one can expect a corresponding increase in the net electron density at the Mn ion sites, resulting in increased occupancy at the e_g orbitals of Mn.

Suntivich et al. [22] further showed that the intrinsic activity of all the oxides in oxidation-reduction reactions exhibits a volcano shape as a function of the e_g-filling of B ions. Assuming that the O_2 molecule probably adsorbs on the surface B sites end-on (Fig. 3), the e_g orbital directed towards an O_2 molecule overlaps the O-2p_σ orbital more strongly than the overlap between the t_{2g} and O-2p_π orbitals, suggesting that the filling of e_g rather than t_{2g} of the B-ion should more accurately determine both the energy gained by adsorption/desorption of oxygen on B ions and the activity, if such an adsorption/desorption process was involved in

the rate-limiting step of the reaction.

Introduction of the abnormal valence ions causes a change in the electronic properties, while oxide ion vacancies increase the mobility of oxide ions and then the ionic conductivity. Since oxide ion vacancies may provide sites hosting supplemental oxygen, it also results in a variation of non-stoichiometric compositions, according to the ambient temperature and the oxygen partial pressure [27].

The nature of B-site cations is of paramount importance for the complete oxidation catalysis of unsubstituted perovskites, although the remarkable function of A-site cations has been reported for the partial oxidation catalysis. The charge-compensating defects that are mainly represented by oxide ion vacancies are also important. Introduction and control of these lattice defects can be attained simply by the partial substitution of non-native cations at the A and B sites. The types and amounts of the lattice defects introduced strongly influence the catalytic properties of substituted perovskites, as a consequence of the modifications to mobility and reactivity of lattice oxygen (typically in Co- and Fe-perovskites) or the oxygen-adsorptive properties of the surface (typically in Mn-perovskites) [18].

Catalytic activity of complex oxides correlates well with their enthalpy of formation from elements per 1 mole of oxygen. At first this concept was explained on the basis of the theory of superficial oxygen bond strength—enthalpy of formation dependence [28]. Later it was pointed out that the band gap corresponds to the enthalpy of formation values and catalytic activity must be explained in terms of electronic conductivity [29].

In related studies, various empirical methods for enthalpy of formation assessment for individual and mixed oxides have been suggested. They are based not only on electronegativities of atoms [30, 31] and geometrical characteristics of the later, but also on crystalline structure in general [32]. According to these methods, enthalpy of formation can be found using different empirical formulas that are generally appropriate for related compound series [33].

From the first group of methods it is necessary to consider Aronson's method [30]:

$$\Delta_f H^0\left(\frac{kJ}{mol}\right) = -96{,}5 n_O \left(X' - X_O\right)^2. \quad (1)$$

Where n_O—quantity of oxygen atoms per a formula unit, X is the weighted geometric mean pseudoelectronegativity of oxide-forming elements that can be defined as follows:

$$X' = X_O + \sqrt{\frac{-\Delta_f H\left(Me_k O_n\right)}{96.5k}}. \quad (2)$$

The second group of methods is based on a correlation between enthalpy of formation and structural parameters of the corresponded mixed oxide. Correlations of formation enthalpy and the Goldschmidt factor were proposed for perovskite-type oxides of general formula ABO_3. This geometrical tolerance factor for the ionic model is defined as a relation [32]:

$$t = \frac{r_A + r_O}{\sqrt{2}\left(r_B + r_O\right)}, \quad (3)$$

where r_i—the effective ionic radius of i-th element depending on its oxidation state and coordination number. For an ideal frame, this factor is identically 1. As a rule, the value of the tolerance factor for perovskite oxides lies within $0.82 < t < 1.02$ [33].

Exothermicity of the mixed oxide from two binary formations is proportional to the difference of their acidity. There are various scales of oxides acidity, empirical to a greater or lesser extent. For example, the numerical scale of Duffy and Ingram [34] is based on the shift of the ultraviolet spectrum of a probe incorporated in various oxides. Smith's scale [35] is based on interaction enthalpy of two binary oxides:

$$\alpha = \Delta_f H^0\left(H_2O\right)^{\frac{1}{2}} - \Delta_f H^0\left(M_x O_y\right)^{\frac{1}{2}}. \quad (4)$$

The attempt of various acidity scales unification has led to consideration of acid-base properties of oxides on the based on their electronic structures. Thus an acidic oxide has a strong electronegativity in combination with high chemical hardness, and the basic one—with low above mentioned characteristics. Acid-base properties of oxides are connected to the energetic position of the valence band [36].

4. Comparative Prediction of Catalytic Activity in the Series of Rare-Earth Manganites

4.1. Application of Artificial Neural Networks to Predict Properties of Catalytic Materials

Statistics suggests regression models for modelling a simultaneous dependency of a variable on several other variables. However, there is also a significant class of machine learning methods that fits the same goal—feed-forward neural networks are the most often encountered representatives of artificial neural networks (ANNs). From a statistical viewpoint, feed-forward neural networks in fact compute complicated nonlinear regression models. However, they arose outside statistics and were typically used without any statistical background. This is particularly true for their applications in catalysis. They are more frequent than the applications of all traditional statistical regression models. The area of ANNs is a rather interdisciplinary area, connecting knowledge from computer science, mathematics and biology. This area, which plays a fundamental role in the analysis of experimental data in catalysis, appeared as a consequence of the following influences [37]:

1) Mathematical modelling of neurons and neural systems.
2) Connectionism, which reviews large networks of simple elements changing their state through mutual interactions as a crucial condition for the existence of any intelligence.
3) Difference between the sequential and algorithmic method of information processing in traditional computers, and the parallel and associative way in which information is processed in biological systems, as well as between the digital representation of information used in the former, and the analogue representation typical of the latter.
4) Universal parallel computers and general methods of parallel computation.

Consolidation of all these sources affected the construction of ANNs as distributed computing systems attempting to achieve a greater or smaller part of the functionality characterising biological neural networks.

A significant attribute of ANNs is that, in contrast to the traditional statistical methods, their applicability does not rely on any specific, hard-to-fulfill conditions. The most noticeable example of one-layer networks is perceptrons—the earliest representative of ANNs in the sense outlined above. The multilayer extension of perceptions, multilayer perceptrons (MLP), is the class of ANNs now most often encountered in practical applications [38].

Another very popular kind of multilayer networks is two-layer radial basis function networks [39], which resemble MLP in being used for their ability to approximate remarkably general mappings. Among the one-layer kinds of neural networks, associative memories are sufficiently useful due to their ability to associate high-dimensional input patterns with low-dimensional output pattern [40]. All these networks are typically used as fully connected. Hence, their architecture is uniquely described with the number of neurons in each layer.

The other example is stacked neural networks [41], which linearly combine several fully connected MLP in their output layer. Such optimal linear combinations of MLP have also been employed to compute nonlinear regression models in catalysis [42].

The most valuable peculiarity of MLP is their universal approximation ability. That is, the universal approximation ability of MLP (as well as of some other kinds of neural networks) means that virtually any unknown dependence can be arbitrarily closely approximated by a function computed by some MLP [43]. In catalysis, we are more frequently interested in dependencies of product yields, catalyst activity, degrees of reactant conversion, and product selectivities on the input variables, such as proportions of catalyst components and reaction conditions [37].

It is necessary to have a sufficient amount of experimental data available to acquire a neural network with desirable performance. The structure and other characteristics of the neural network should be optimised to the particular problem under study by the training and testing process. Just after the neural network has become sufficiently trained on the basis of these data, then it becomes workable to generate adequate results when submitted with any new input data it has never experienced before. The training process includes minimising the sum of square error between real and predicted outputs, put in practice the available training data, by continuously adjusting and subsequently determining the weights connecting neurons in adjacent layers [38].

The quantity of neurons in the hidden layer multiplies the sums of connections and weights to be fitted. This number cannot be increased without limit, because may reach a state where the quantity of the connections to be fitted is larger than the quantity of the data available for training. Even if the neural network can still be trained, the case is mathematically undetermined. Mathematically it is not permissible to define more fitting parameters than the available data points. Neural network modelling should be practiced with exceptional care regarding sufficient data to be efficient [44].

As a rule, the linear correlations between enthalpies of formation and characteristics of the perovskite oxides are assumed. Meanwhile, there are no reasons to state which type of approximation is exactly the best due to the absence extensive theoretical knowledge and only empirical correlations usage [30, 32, 45]. We suggest using a combination of both groups of methods by the instrumentality of ANNs. In the light of this problem the following ANN advantages in comparison with conventional approximation should be emphasized [46]: 1) low sensitivity to noisy and incomplete input data and 2) no prior knowledge about a kind of dependence of the target variables on the inputs is required.

In this work ANN will be applied for the purpose of simultaneous inclusion of several parameters in a predictive model. Thus, the kind of input variable—target variable dependence is being defined only during the training process that is much better than finding linear correlations with each parameter independently.

4.2. ANN Training Procedure

Before ANN building, the first task to be solved is to choose the most informative input variables (descriptors). The number of descriptors must be restricted to those with a clear physicochemical meaning (with the purpose of avoiding complex stochastic methods) [47], the following descriptors were chosen under this guidance:

1) Smith's acidity difference of constituent oxides,

$$\alpha_{A_kO_l} - \alpha_{B_mO_n} = \sqrt{\Delta_f H^0_{B_mO_n}} - \sqrt{\Delta_f H^0_{A_kO_l}} \,. \quad (5)$$

2) Electronegativity difference of constituent oxides,

$$X_{A_kO_l} - X_{B_mO_n} = \left(X_A^k X_O^l\right)^{\frac{1}{k+l}} - \left(X_B^m X_O^n\right)^{\frac{1}{m+n}} . \quad (6)$$

3) The tolerance factor for given mixed oxide (t from Eq. (3)).

Thus, all the descriptors characterize energetics of mixed oxide formation as a result of acid-base chemical reaction of constituent oxides with each other. The descriptors were calculated with the usage of the reference values of Pauling electronegativity, ionic radii, and enthalpies of formation for binary oxides. Experimental enthalpies of formation for the perovskite-type mixed oxides were taken from the latest publications concerning this issue [4, 33, 45]. We considered only perovskites where the A atom is a group 2 element or trivalent lanthanide metal and the B atom is one of d- or f-elements. Enthalpies of acid-base chemical reaction of constituent oxides with each other were chosen as a dependent variable and calculated as follows:

$$\Delta_r H^0 = \Delta_f H^0_{ABO_3} - \frac{1}{k}\Delta_f H^0_{A_kO_l} - \frac{1}{m}\Delta_f H^0_{B_mO_n} . \quad (7)$$

The problem of choosing the ANN optimum architecture has been solved by training various MLP with one hidden layer of neurons. The presence of only one hidden layer is caused by the small dimension of a training sample. However according to Hecht-Nielsen theorem [48] any continuous multivariable function can be approximated by the feed-forward neural network with one hidden layer with an adequate quantity of hidden units and a single linear output unit. According to the theorem of completeness, any continuous function on the closed array can be regularly approached via the functions calculated by neural networks, if the activation function of a neuron is twice continuously differentiable and continuous [49]. The hyperbolic tangent (sigmoid) is chosen as an activation function for neurons of the hidden layers under this guidance.

The input layer consists of three neurons corresponding to each explanatory variable, the target one consists of a neuron corresponding to the dependent variable (Fig. 4). The percep-

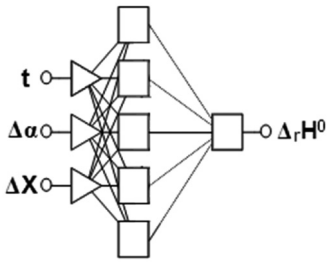

Fig. 4. The architecture of the artificial neural network used.

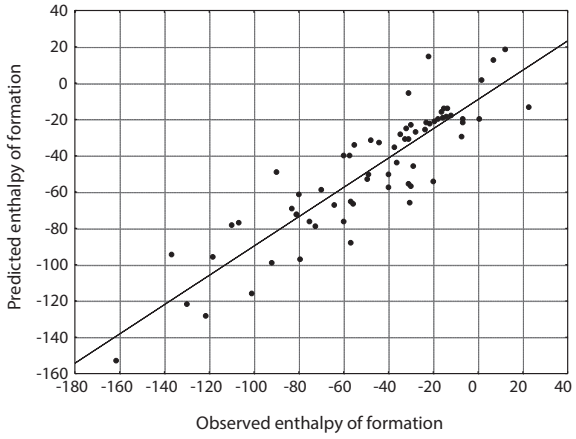

Fig. 5. Results of artificial neural network ensemble training.

trons were being trained with various quantities of neurons in the hidden layer using a training sample—matrix consisting of 75 rows and four columns of data. The training process included minimization of the sum of squared errors between experimental data and predicted values using network synaptic weights fitting the connected neurons of adjacent ANN layers.

Training performance was supervised on an independent sample (cross-validation). For ANN training, the sequence of 100 iterations on the backpropagation algorithm was used with the subsequent use of Broyden-Fletcher-Goldfarb-Shanno (BFGS) algorithm (quasi-Newton). The whole training dataset for each neural network was randomly divided into training, cross-validation and test samples in the ratio 4:1:1, respectively. An early stop method was chosen as a stopping criterion for training. Training results determined the number of hidden neurons equals 5, as priority should be given to the simplest ANN architecture. Increasing the quantity of neurons in the hidden layer directly increases the quantity of network weights to be optimized, that demands multiplication of training sample or leads to the loss of ANN generalization ability. After the optimum quantity of neurons in the hidden layer was established, 20,000 three-layer perceptrons of architecture 3-5-1 with different initial synaptic weights were trained based of the above-stated procedure.

4.3. Comparison of Catalytic Activity in the Series of Rare-Earth Manganites

After training 5 the most successfully trained ANNs have been collected into the entrance ensemble for making predictions. Experimental values of the enthalpy of mixed oxide formation from constituent oxides have been compared to the predicted values (Fig. 5). Observing the linear relationship between these variables, we can conclude that experimental enthalpies of formation and the enthalpies calculated by the ANN ensemble are in good agreement.

Table 1 summarizes the data obtained for the enthalpy of constituent oxides reaction ($\Delta_r H^0$), reference data [50] for the enthalpy of rare-earth binary oxides formation ($\Delta_f H^0_{Ln_2O_3}$), calculated data for the enthalpy of rare-earth perovskites formation ($\Delta_f H^{0,calc}_{LnMnO_3}$) and results estimated by Yokokawa et al. [32], based on the effective radii approach (enthalpies are given in kJ/mol).

Reference data for some other relevant rare-earth manganites are experimentally defined and collected in Table 2.

The more exothermic the reaction of mixed oxide formation is, the less catalytic activity the later can possess in oxidation reactions. We can conclude that the catalytic activity of the perovskites decreases in the following series: $EuMnO_3$ > $CeMnO_3$ > $PrMnO_3$ > $SmMnO_3$ > $LaMnO_3$ > $DyMnO_3$.

From this series, it is obvious that europium manganite, with the least negative formation enthalpy, should possess the greatest catalytic activity, and cerium manganite should be worse in this quality. However it is necessary to mention some advantages of practical application of the later (its ability not only to exhibit stable oxidation states +3 and +4 but also to possess oxygen buffer properties). The cost of each rare-earth manganite includes

Table 1. Enthalpies of rare-earth manganites formation predicted by artificial neural network

Substance	$\Delta_f H^0_{Ln_2O_3}$	$\Delta_f H^{0,calc}_{LnMnO_3}$	$\Delta_f H^{0,ref}_{LnMnO_3}$	$\Delta_r H^0$
$CeMnO_3$	-1799.8	-1403	-1422.6	-24
$PrMnO_3$	-1809.9	-1403	-1850.1	-20
$EuMnO_3$	-1662.5	-1358	-1335.9	-48
$GdMnO_3$	-1854.0	-1428	-1416.0	-22
$TbMnO_3$	-1865.2	-1427	-1432.6	-15
$HoMnO_3$	-1883.3	-1445	-1437.9	-25
$TmMnO_3$	-1889.3	-1443	-1437.9	-19

Table 2. Reference enthalpies of some rare-earth manganites formation

Substance	$\Delta_f H^{0,ref}_{LnMnO_3}$ (kJ/mol)
$LaMnO_3$	-1,425.1
$NdMnO_3$	-1,442.1
$SmMnO_3$	-1,423.4
$DyMnO_3$	-1,426.7
$ErMnO_3$	-1,444.4
$YMnO_3$	-1,449.1

Table 3. Current price of the most environmentally prospective rare-earth oxides

Substance	Price (USD/kg)
Eu_2O_3	965.0
Ce_2O_3	22.0
Pr_2O_3	56.0
Sm_2O_3	52.6
La_2O_3	24.0
Dy_2O_3	450.0

cost or rare-earth oxide as a precursor; the prices of the aforementioned binary rare-earth oxides [51] are summarized in Table 3.

Looking through these data we can conclude that cerium manganite is the most feasible for industrial usage due to the fact that it is more than ten times cheaper compared to europium manganite.

5. Conclusions

Rare-earth manganites have a high potential for applications based on their physico-chemical properties. The catalytic activity is associated with the enthalpy of formation and the possibility of oxygen vacancies formation in the solid. ANNs were used to predict the enthalpies of formation for a series of rare-earth manganites. A comparison of the enthalpies of formation of perovskites shows that europium, cerium, praseodymium, and samarium manganites must be the most active in oxidation reactions. The present study has shown that cerium manganite is the most feasible for industrial oxidation processes. This conclusion is in good agreement with contemporary practice of cerium manganite and related compounds usage in environmental catalysis. Further improvement of the catalyst can be reached by the addition of other transitional metals and oxygen vacancies forming.

Development of excellent new catalysts is always one of the aims of catalytic research. Although catalytic studies so far have been conducted largely on somewhat A-site-substituted perovskites, B-site replacement has been known to exhibit an evenly powerful or synergetic consequence in some cases. Suitable compositions of perovskites with mixed cations at both A- and B-site will open the door to much better catalysts. From an activity point of view, it can be said that the preparation of perovskites in the form of fine particles, pure or supported, is also primary to meet the needs in practical applications. Expectations remain high regarding new discoveries of excellent perovskite catalysts and fascinating new reactions catalyzed by perovskites, since perovskites offer a wide range of possibilities in tailoring chemical and physical properties.

References

1. Centi G, Ciambelli P, Perathoner S, Russo P. Environmental catalysis: trends and outlook. *Catal. Today* 2002;75:3-15.
2. Pena MA, Fierro JL. Chemical structures and performance of perovskite oxides. *Chem. Rev*. 2001;101:1981-2018.
3. Abordeoaei L, Papp HI. Perovskite utilisation as catalysts in NO reduction by SCR-HC in absence of O_2. *Environ. Eng. Manag. J*. 2004;3:755-760.
4. Laberty C, Navrotsky A, Rao CN, Alphonse P. Energetics of rare earth manganese perovskites A1–xA´xMnO$_3$ (A=La, Nd, Y and A´=Sr, La) systems. *J. Solid State Chem*. 1999;145:77-87.
5. Uemura S, Mitsudo T, Haruta M, Inui T. Frontiers and tasks of catalysis towards the next century. Proceedings of the International Symposium in honour of Professor Tomoyuki Inui. Utrecht: VSP; 1998.
6. Isupova LA, Sadykov VA, Solovyova LP, et al. Monolith perovskite catalysts of honeycomb structure for fuel combustion. *Stud. Surf. Sci. Catal*. 1995;91:637-645.
7. Spinicci R, Faticanti M, Marini P, De Rossi S, Porta P. Catalytic activity of $LaMnO_3$ and $LaCoO_3$ perovskites towards VOCs combustion. *J. Mol. Catal. A Chem*. 2003;197:147-155.
8. Chirila LM, Papp H, Suprun W, Balasanian I. Synthesis, characterization and catalytic reduction of NO_x emissions over $LaMnO_3$ perovskite. *Environ. Eng. Manag. J*. 2007;6:549-553.
9. Yonghua C, Futai M, Hui L. Catalytic properties of rare earth manganites and related compounds. *React. Kinet. Catal. Lett*. 1988;37:37-42.
10. Liu Y, Dai H, Du Y, et al. Controlled preparation and high catalytic performance of three-dimensionally ordered macroporous $LaMnO_3$ with nanovoid skeletons for the combustion of toluene. *J. Catal*. 2012;287:149-160.
11. Li C, Lin Y. Methanol partial oxidation over palladium-, platinum-, and rhodium-integrated $LaMnO_3$ perovskites. *Appl. Catal. B* 2011;107:284-293.
12. Zhang C, Wang C, Zhan W, et al. Catalytic oxidation of vinyl chloride emission over $LaMnO_3$ and $LaB_{0.2}Mn_{0.8}O_3$ (B=Co, Ni, Fe) catalysts. *Appl. Catal. B* 2013;129:509-516.
13. Ran R, Wu X, Quan C, Weng D. Effect of strontium and cerium doping on the structural and catalytic properties of $PrMnO_3$ oxides. *Solid State Ion*. 2005;176:965-971.
14. Tang X, Li Y, Huang X, et al. MnO_xCeO_2 mixed oxide catalysts for complete oxidation of formaldehyde: effect of preparation method and calcination temperature. *Appl. Catal. B* 2006;62:265-273.
15. Liu J, Zhao Z, Xu C. Research progress in catalysts for removal of soot particulates from diesel engines. *Chin. J. Catal*. 2004;25:673-680.
16. Raj SL, Srinivasan V. Decomposition of nitrous oxide on rare earth manganites. *J. Catal*. 1980;65:121-126.
17. Lombardo EA, Ulla MA. Perovskite oxides in catalysis: past, present and future. *Res. Chem. Intermed*. 1998;24:581-592.
18. Arai H, Yamada T, Eguchi K, Seiyama T. Catalytic combustion of methane over various perovskite-type oxides. *Appl. Catal*. 1986;26:265-276.
19. Lintz HG, Wittstock K. Catalytic combustion of solvent containing air on base metal catalysts. *Catal. Today* 1996;29:457-461.
20. Luna AJ, Rojas LOA, Melo DMA, Benachour M, Sousa JF. Total catalytic wet oxidation of phenol and its chlorinated derivates with MnO_2/CeO_2 catalyst in a slurry reactor. *Braz. J. Chem. Eng*. 2009;26:493-502.
21. Zhou G, Shah PR, Gorte RJ. A study of cerium-manganese mixed oxides for oxidation catalysis. *Catal. Lett*. 2008;120:191-197.
22. Suntivich J, Gasteiger HA, Yabuuchi N, Nakanishi H, Goodenough JB, Shao-Horn Y. Design principles for oxygen-reduction activity on perovskite oxide catalysts for fuel cells and metal-air batteries. *Nat. Chem*. 2011;3:546-550.
23. Rezlescu N, Rezlescu E, Doroftei C, Popa PD, Ignat M. Nanostructured lanthanum manganite perovskites in catalyst applications. *Dig. J. Nanomater. Biostruct*. 2013;8:581-587.
24. Arakawa T, Yoshida A, Shiokawa J. The catalytic activity of rare earth manganites. *Mater. Res. Bull*. 1980;15:269-273.
25. Yamazoe N, Teraoka Y. Oxidation catalysis of perovskites: relationships to bulk structure and composition (valency, defect, etc.). *Catal. Today* 1990;8:175-199.
26. Voorhoeve RJ, Johnson DW Jr, Remeika JP, Gallagher PK. Perovskite oxides: materials science in catalysis. *Science* 1977;195:827-833.
27. Kalashnikova AM, Pisarev RV. Electronic structure of hexagonal rare-earth manganites $RMnO_3$. *J. Exp. Theor. Phys. Lett*.

2003;78:143-147.
28. Moro-Oka Y, Morikawa Y, Ozaki A. Regularity in the catalytic properties of metal oxides in hydrocarbon oxidation. *J. Catal*. 1967;7:23-32.
29. Vijh AK, Lenfant P. Significance of heterogeneous catalysis of certain oxidation reactions by oxides in relation to their heats of formation. *Can. J. Chem*. 1971;49:809-812.
30. Aronson S. Estimation of the heat of formation of refractory mixed oxides. *J. Nucl. Mater*. 1982;107:343-346.
31. Vonka P, Leitner J. A method for the estimation of the enthalpy of formation of mixed oxides in Al_2O_3–Ln_2O_3 systems. *J. Solid State Chem*. 2009;182:744-748.
32. Yokokawa H, Kawada T, Dokiya M. Thermodynamic regularities in perovskite and K_2NiF_4 compounds. *J. Am. Ceram. Soc*. 1989;72:152-153.
33. Stolen S, Grande T. Chemical thermodynamics of materials: macroscopic and microscopic aspects. Hoboken: John Wiley and Sons; 2004.
34. Duffy JA, Ingram MD. Establishment of an optical scale for Lewis basicity in inorganic oxyacids, molten salts, and glasses. *J. Am. Ceram. Soc*. 1971;93:6448-6454.
35. Smith W. An acidity scale for binary oxides. *J. Chem. Educ*. 1987;64:480-481.
36. Portier J, Poizot P, Campet G, Subramanian MA, Tarascon JM. Acid-base behavior of oxides and their electronic structure. *Solid State Sci*. 2003;5:695-699.
37. Baerns M, Holena M. Combinatorial development of solid catalytic materials: design of high-throughput experiments, data analysis, data mining. London: Imperial College Press; 2009.
38. Jain AK, Mao J, Mohiuddin KM. Artificial neural networks: a tutorial. *IEEE Computer* 1996;29:31-44.
39. Buhmann MD. Radial basis functions: theory and implementations. New York: Cambridge University Press; 2003.
40. Hassoun MH. Fundamentals of artificial neural networks. Cambridge: MIT Press; 1995.
41. Sridhar DV, Seagrave RC, Bartlett EB. Process modeling using stacked neural networks. *AIChE J*. 1996;42:2529-2539.
42. Tompos A, Margitfalvi JL, Tfirst E, Vegvari L. Information mining using artificial neural networks and "holographic research strategy". *Appl. Catal. A* 2003;254:161-168.
43. Burden FR. Mapping analytic functions using neural networks. *J. Chem. Inf. Comput. Sci*. 1994;34:1229-1231.
44. Sha W, Edwards KL. The use of artificial neural networks in materials science based research. *Mater. Des*. 2007;28:1747-1752.
45. Dash S, Singh Z, Parida SC, Venugopal V. Thermodynamic studies on Rb_2ThO_3(s). *J. Alloys Compd*. 2005;398:219-227.
46. Diaconescu R, Dumitriu E. Applications of artificial neural networks in environmental catalysis. *Environ. Eng. Manag. J*. 2005;4:473-498.
47. Rothenberg G. Data mining in catalysis: separating knowledge from garbage. *Catal. Today* 2008;137:2-10.
48. Hecht-Nielsen R. Replicator neural networks for universal optimal source coding. *Science* 1995;269:1860-1863.
49. Sontag ED. Feed forward nets for interpolation and classification. *J. Comput. Sys. Sci*. 1992;45:20-48.
50. Morss LR, Konings RJM. Thermochemistry of binary rare earth oxides. Dordrecht: Kluwer Academic Publishers, 2006.
51. Available from: http://www.alibaba.com.